© 2015. Published by The Company of Biologists Ltd | Journal of Experimental Biology (2015) 218, 3164-3174 doi:10.1242/jeb.103937

REVIEW

Cleanliness is next to godliness: mechanisms for staying clean

Guillermo J. Amador[1] and David L. Hu[1,2,*]

ABSTRACT

Getting dirty is a fundamental problem, and one for which there are few solutions, especially across the enormous range of animal size. How do both a honeybee and a squirrel get clean? In this Review, we discuss two broad types of cleaning, considered from the viewpoint of energetics. Non-renewable cleaning strategies rely upon the organism as an energy source. Examples include grooming motions, wet-dog shaking or the secretion of chemicals. Renewable cleaning strategies depend on environmental sources of energy, such as the use of eyelashes to redirect incoming wind and so reduce deposition onto the eye. Both strategies take advantage of body hair to facilitate cleaning, and honeybees and squirrels, for example, each have around 3 million hairs. This hair mat increases the area on which particles can land by a factor of 100, but also suspends particles above the body, reducing their adhesion and facilitating removal. We hope that the strategies outlined here will inspire energy-efficient cleaning strategies in synthetic systems.

KEY WORDS: Filter, Bristles, Evolution, Soiling, Fouling, Cleaning

Introduction

As their surroundings change, organisms survive by maintaining stable internal and external states. Their internal state is characterized by temperature, salinity and pH, whose regulation has been well studied (Schmidt-Nielsen, 1984). Equally important, but less quantified, is an organism's external state. This state involves an animal's surface – its interface with the outside world. A poorly maintained surface can lead to the transmission of bacteria, disease, parasites such as mites and ticks, and the obstruction of visual, auditory and olfactory organs. How do organisms fend off such a large range of intruders? The goal of this Review is to present a mathematical and physical framework for understanding the ways in which animals stay clean. We avoid complex mathematics, but aim to be quantitative using scaling. This approach takes into account the size and geometry of the organism, and facilitates comparison of organisms of a range of sizes.

The act of cleaning, both in nature and our everyday lives, is defined by the removal and relocation of accumulated debris. Such debris is often in the form of dust, pollen, and liquid droplets that readily adhere to a wide range of surfaces. To clean such debris, energy is needed. The source of this energy enables us to define two broad categories of cleaning, listed in Table 1. If an organism expends its own energy, it carries out non-renewable cleaning. Specialized grooming movements, for example, are driven by muscular energy. An organism uses its own energy to groom, lick, wet-dog shake or secrete bactericides. To each of these movements, there exists an analogy in the built world. We vacuum carpets, wipe tabletops, spin-dry our clothes and spray chemicals to kill bacteria. Since such methods rely upon limited resources, care must be taken to minimize their use.

An organism performs renewable cleaning if it relies upon its surroundings for energy. This is the ideal strategy because such energy is effectively unlimited. The eyelashes of mammals deflect incoming wind, curving the trajectory of particles before they can deposit onto the eye surface. The hairs between the ommatidia of insect compound eyes do the same thing. Lotus leaves have microscopic bumps that make their surfaces super-hydrophobic, allowing raindrops to pick up debris as they roll off. Nano-scale posts on cicada wings can puncture and kill bacteria. All of these cleaning methods are driven by energy from the organism's surroundings. Regrettably, human-made cleaning mechanisms rely mostly upon non-renewable strategies. One of the goals of this Review is to attract attention to opportunities in renewable cleaning strategies so a greater number of energy-efficient solutions can be developed.

In this Review, we discuss the biology and physics of cleaning in nature. We begin by characterizing the types of particles in the environment and their effect on organisms and devices. The rest of this Review pertains mostly to organisms, focusing on insects. We proceed by measuring the susceptibility of organisms to accumulation of particles. To do so, we calculate the true surface areas of organisms, which may be 100 times greater than their apparent surface area. By 'hair', we refer generally to any elongate structures such as setae, combs and brushes. In the next section, we present mathematical formulae for adhesion forces of particles, including capillary, van der Waals, electrostatic and claw-gripping forces. We will use these forces to provide a baseline force for particle removal. Lastly, we summarize our physical approach to cleaning, emphasizing the new approaches that we have identified.

Environmental particles and their effect on organisms and devices

Airborne debris may be wet or dry. In this section, and throughout the Review, we refer to airborne aerosols, both dry and wet, as particles. Airborne particles have a trimodal size distribution, with peaks at particle sizes of 0.01, 0.5 and 10 µm (Wilson et al., 1977). These particles consist mostly of dust from roads, construction, crops and livestock, and emissions from fires, fuel combustion and industrial processes (US Environmental Protection Agency, 2014). As human populations and the demand for energy, transportation, food and technologies increase, so do the concentrations of particulates in the atmosphere. Between 1993 and 2003, the concentration of particles sized 10 µm and below increased by 28% (US Environmental Protection Agency, 2013). Little is known about how animals have adapted to this dramatic change in particulates.

Typical particles that animals must contend with are shown in Fig. 1. The small size of dust and pollen (Fig. 1A,D) may make it seem harmless to humans, notwithstanding allergies. However, for smaller animals, like insects, continual accumulation can reduce

[1]School of Mechanical Engineering, Georgia Institute of Technology, 801 Ferst Drive, MRDC 2211, Atlanta, GA 30332, USA. [2]School of Biology, Georgia Institute of Technology, 310 Ferst Drive, Atlanta, GA 30322, USA.

*Author for correspondence (hu@me.gatech.edu)

Journal of Experimental Biology

Journal of Experimental Biology (2015) 218, 3164-3174 doi:10.1242/jeb.103937

Table 1. Classification of cleaning strategies found in nature and human-made devices

	Method in nature	Equivalent method in humans
Non-renewable cleaning strategy	Hair flicking	Vacuuming with agitator brush
	Shearing wet footpads, licking with tongue	Washing with wet cloth
	Brushing with bristled appendages	Sweeping with broom
	Wet-dog shake	Spin-drying in laundry machines
	Shearing gecko feet setae	Cleaning brushes
	Fluid secretion of chemical bactericides	Antibacterial coatings
Renewable cleaning strategy	Ocular hairs, eyelashes	Compressed air to blow dust from laptops
	Lotus effect	Hydrophobic paints
	Cicada wing posts, or geometric bactericides	To be invented
	Smooth leaves cleaned by the wind	To be invented

maneuverability or occlude sensory organs. A typical honeybee, which forages for pollen, accumulates up to 30% of its body mass in pollen in one trip and up to five times its body mass in one day of foraging (Winston, 1991). If pollen were not regularly cleaned from the bee's antennae, eyes and wings, controlled flight would be impossible. Hairs covering the honeybee, like those shown in Fig. 2, are thought to facilitate the removal of accumulated pollen (Thorp, 1979). Living particles such as *Varroa* (Fig. 1B,E) and tracheal mites can harm honeybees if not removed quickly (Sammataro et al., 2000; Villa, 2006). Dew and fog can accumulate to such large masses that they overwhelm small insects, as shown in Fig. 1C,F. The largest water drop that can be sustained by surface tension would add about 80 mg of mass to a mosquito – about 80 times its mass! A single water drop with a diameter of only 0.6 mm would weigh the same as a mosquito. For all of these cases, the controlled accumulation and removal of particles is an important part of an animal's survival in a particle-laden environment.

The accumulation of certain particles can lead to disease. Drops expelled during coughing or sneezing can spread respiratory diseases to humans meters away (Bourouiba et al., 2014). The dangers of disease transmission through fluid exchange were made apparent during the 2014 outbreak of the Ebola virus in West Africa and its spread to Europe and the US. The rapid spread of the virus demonstrated the paramount importance of effective methods for limiting the spread of fluid particles. Mites, ticks and fleas can spread to other animals through contact. Mite-associated viral pathologies threaten the survival of captive and feral honeybees, which play a critical role in the pollination of many of our agricultural plants (Sammataro et al., 2000). Understanding how organisms contend with such virulent particles has implications in the ecology of disease transmission.

As in animals, many human-made technologies are prone to soiling, especially when operating in nature. Accumulation of particles is particularly important for the maintenance of remote sensing applications, such as for autonomous robots, which cannot be easily accessed once deployed (Mazumder et al., 2003; Calle et al., 2008). Photovoltaic solar panels also accumulate dust, which results in annual reductions in efficiency of 6% (Kumar and Sarkar, 2013).

An animal's surface area

Just as a coastline experiences the rising tide, an animal's surface experiences soiling. In typical calculations of surface area to predict heat loss, only the area of the skin is considered. However, both skin and hair are susceptible to deposition of particles. The surface area of the skin (A_{body}) and hairs (A_{hair}) are shown schematically in Fig. 3A.

We begin by calculating the apparent surface area of an animal. The surface area of an animal's skin can be approximated by assuming it is cylindrical, or $A_{body} \approx \pi D_b L_b$, where D_b is the diameter of the animal's body and L_b is its length. If an object is enlarged, but maintains the same proportions, its surface area follows the isometric relationship $A \sim V^{2/3}$ (McGowan, 1994) where V is the animal's volume. This is clearly true for spheres

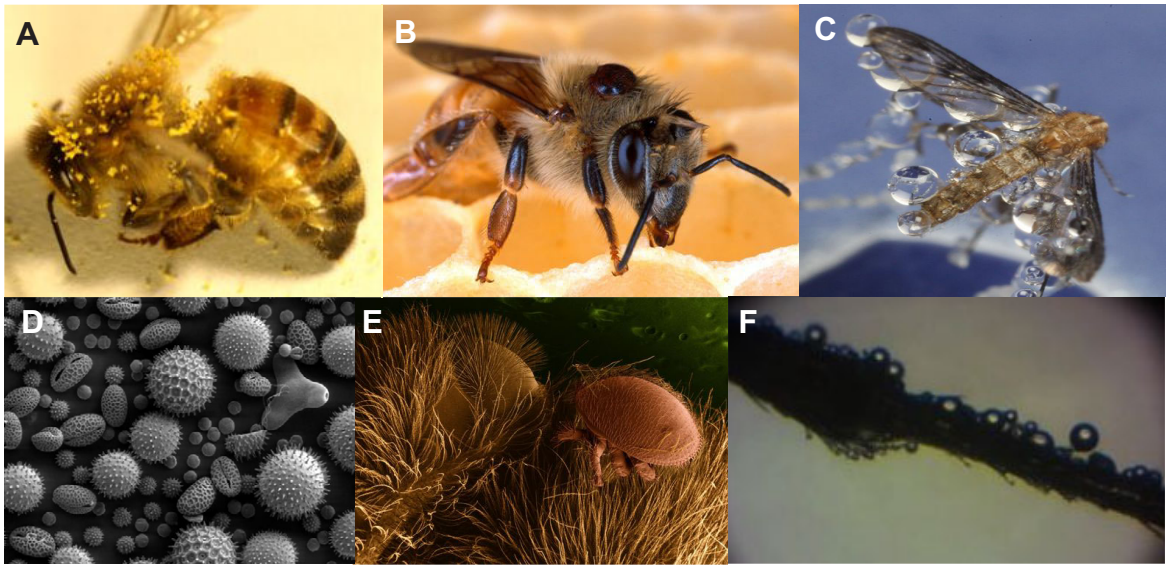

Fig. 1. Soiling of insects. (A) A honeybee covered with pollen. (B) A honeybee with a *Varroa* mite on its thorax. (C) A mosquito with dew droplets accumulated. (D) A variety of pollen. (E) A *Varroa* mite on the thorax of a honeybee. (F) A mosquito leg covered in dew. Photo credit: (B,D,E) Wikimedia Commons.

Journal of Experimental Biology (2015) 218, 3164-3174 doi:10.1242/jeb.103937

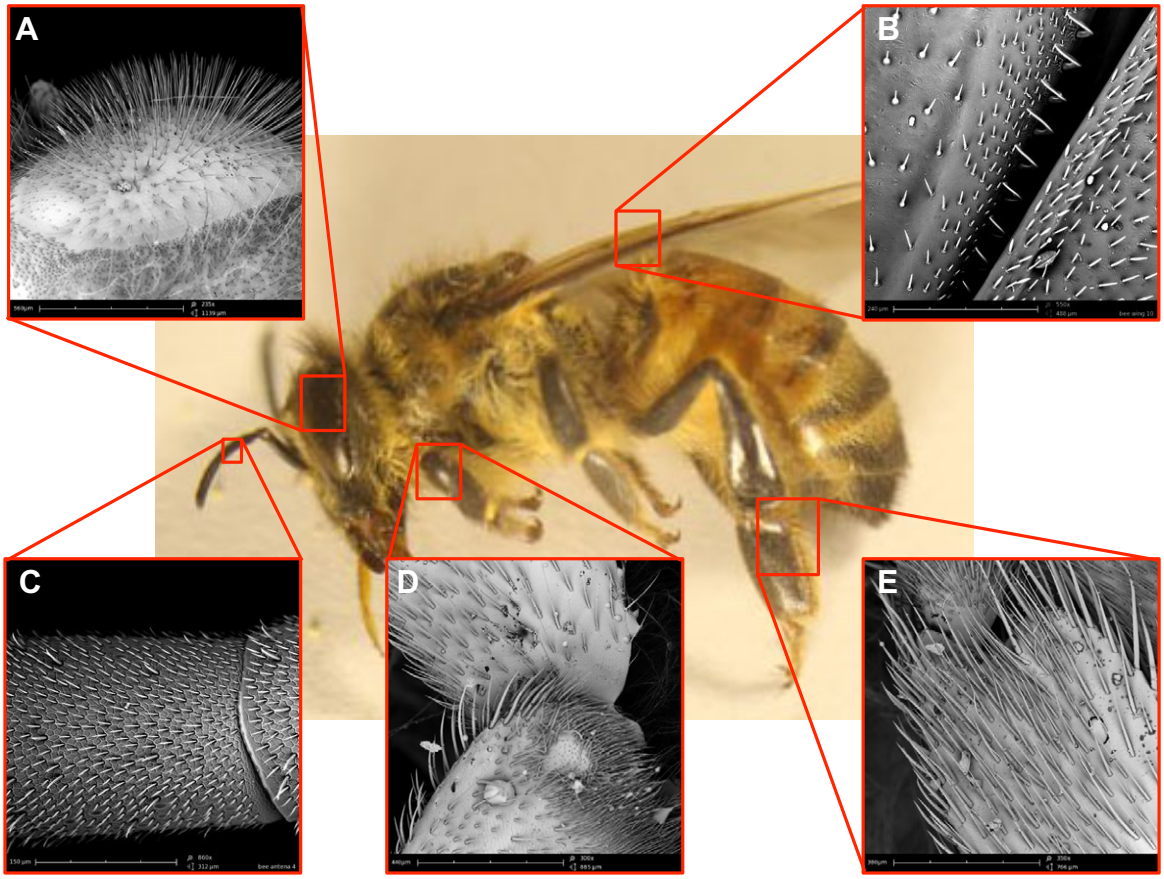

Fig. 2. Grooming structures and their targets on the honeybee. SEM images of hairs on a honeybee's (A) eye, (B) wing, (C) antenna, (D) forelimb and (E) hindlimb. (B–C) from Anne Marie Maes (annemariemaes.net; SEM images recorded at the Department of Materials and Chemistry, Vrije Universiteit Brussel, Belgium).

and cubes, as well as any other shape. Thus, isometry is a good assumption for sets of animals that have the same proportion. Eutherian mammals and salamanders have a skin surface area A_{body} that is consistent with isometry, or $A_{body}{\sim}M_b^{2/3}$ where M_b is body mass (McMahon et al., 1983; Calder, 1996). Similarly, for the 27 mammals and insects shown in Fig. 3B, we see that $A_{body}{\sim}M_b^{0.53}$. Since this exponent is less than unity, we conclude that as animals shrink, their surface area to volume ratio increases. This increased surface area makes small animals increasingly susceptible to soiling.

An animal's hairs can make its true surface area in great excess of its apparent surface area. We model a single hair as a cone, shown schematically in Fig. 3A with a basal diameter h and length L. The animal has η hairs per unit area. The true surface area of an animal, A_{hair}, may be written as the number of hairs, $A_{body}\eta$, multiplied by each hair's surface area contribution, yielding:

$$A_{hair} = \frac{\pi}{2} h \sqrt{L^2 + \frac{h^2}{4}} A_{body}\eta. \quad (1)$$

We may determine how true surface area changes with body size by measuring hair spacing and geometry. We do so with 17 mammals (Wilcox, 1950; McManus, 1974; Jenkins and Busher, 1979; Estes, 1980; Willner et al., 1980; Olsen, 1983; Conley and Porter, 1986; Pass and Freeth, 1993; Koprowski, 1994; Larivière and Walton, 1998; Pasitschniak-Arts and Marinelli, 1998; Sidorovich et al., 1999; Mattern and McLennan, 2000; Scott et al., 2001; Fish et al., 2002; Valencak et al., 2003; Spotorno et al., 2004; Fedosenko and Blank, 2005; Mecklenburg et al., 2009; Dickerson et al., 2012) and 10 insects (Carlson and Chi, 1974 and data from a range of online SEM images). These measurements yield scalings given in Table 2. Hair diameter h is shown in Fig. 4A, whose best fit gives $h{\sim}M_b^{0.081}$. The optimal hair diameter for minimizing convective heat loss was found analytically by Bejan to be $h{\sim}M_b^{1/12}{\sim}M_b^{0.083}$ (Bejan, 1990), which is well within the 95% confidence interval. Therefore, body hair may be optimized to provide heat insulation. Hair length L is shown in Fig. 4B, and scales as $L{\sim}M_b^{0.35}$, which is within the 95% confidence interval of isometry, $L{\sim}M_b^{1/3}$. Hair density η is shown in Fig. 4C and scales as $\eta{\sim}M_b^{-0.34}$. All together, we find $A_{hair}{\sim}M_b^{0.63}$.

The red squares and blue crosses in Fig. 3B refer to the apparent and true surface area of an animal, respectively. The contribution of the hairs is undeniable: an animal's hairy surface area can exceed 100 times the surface area of its skin. This factor appears accurate across 12 orders of magnitude in body size. Consideration of the true surface areas of typical organisms can be striking. A honeybee has a surface area of 70 cm^2, the area of a slice of toast. A cat has a surface area of 3 m^2, the area of a ping-pong table. This number explains why bathing a pet never seems to get it perfectly clean. Both apparent and true surface area scale similarly with body mass, with power law exponents within 16% of each other: 0.53 and 0.63, respectively. The expected coefficient of 0.67 is within the 95% confidence interval for the surface area of hair.

The total number of hairs N is a dimensionless number that can be used to visualize how hairy these animals are. The total number of hairs may be written as $N{=}\eta A_{body}{\sim}M_b^{0.20}$ and is shown in Fig. 3C. Of

Journal of Experimental Biology

Journal of Experimental Biology (2015) 218, 3164-3174 doi:10.1242/jeb.103937

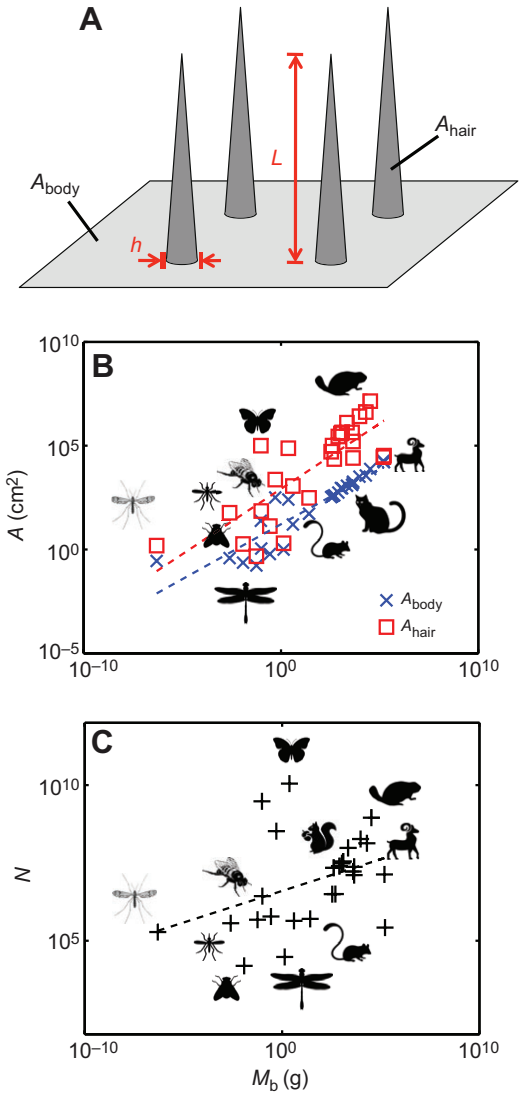

Fig. 3. Hair increases the surface area susceptible to soiling. (A) Schematic of a hairy surface showing hair basal diameter, *h*, and length, *L*. (B) Relationship between surface area and animal body mass. The red boxes show the true surface area (A_{hair}) of an animal including its hair; the blue crosses show the apparent surface (A_{body}) of the animal, if it were shaved. Dashed lines represent curves of best fit. (C) Relationship between total number of hairs and animal body mass. Best fit curves are given by dashed lines, whose equations are presented in Table 2.

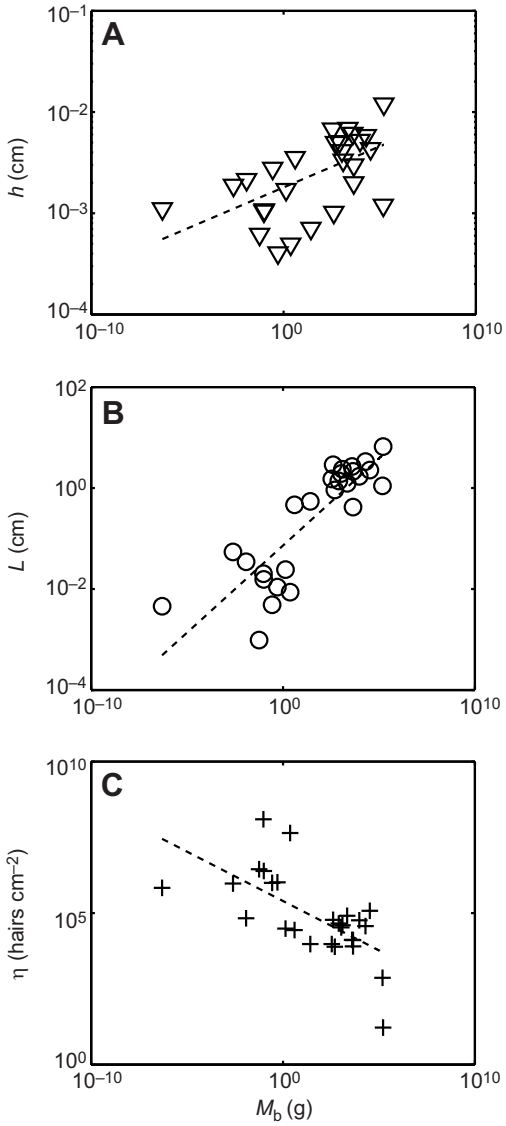

Fig. 4. Parameters for calculating total surface area. (A) Relationship between hair thickness and animal body mass. (B) Relationship between hair length and animal body mass. (C) Relationship between hair density in number of hairs per cm^2 and animal body mass. Best-fit curves are given by dashed lines, whose equations are presented in Table 2.

the animals studied, the hairstreak butterfly and luna moth are the hairiest, with 10^{10} hairs, roughly an order of magnitude greater than the beaver and sea otter. In comparison, the human head has only 10^5 hairs. The butterfly's great number of hairs is made possible by an extremely high hair density, three orders of magnitude greater than the beaver. Thus, body size can often be misleading when considering which animal has more hairs. Another example is the honeybee, which is as hairy as a grey squirrel, each with just over 3 million hairs, despite the bee being three orders in magnitude smaller in mass. A greater number of hairs indicates a greater susceptibility to soiling.

Why then are animals so hairy? Hair serves a multitude of functions. Hairs provide insulation to help with temperature regulation in mammals (Bejan, 1990). Hairs on the footpads of animals provide adhesion for locomotion (Autumn et al., 2002; Federle, 2006). At small length scales and high densities, arrays of hairs can even replace solid surfaces. Such is the case for small flying insects called thrips (Sato et al., 2013). High-density arrays of hairs may aid in chemoreception in moths (Vogel, 1983), and airflow sensing in crickets (Casas et al., 2010) and honeybees (Neese, 1965, 1966). Hairs on insects can also increase their water repellency, which is important for flying, terrestrial and water-walking insects (Holdgate, 1955). Nevertheless, the more hairs, the more places for particles to become attached. In the next section, we calculate the attachment force of these particles.

Particle adhesion

Particles are often removed by shaking or flicking. By Newton's second law, a particle of mass M_p attached to an animal by an adhesive force F must be shaken at an acceleration $a \geq (F/M_p)$ to be ejected using its own inertia. Thus, for a given adhesion force, a smaller particle is harder to shake off. From here on, as a proxy for attachment force, we consider the acceleration a required to

Journal of Experimental Biology (2015) 218, 3164-3174 doi:10.1242/jeb.103937

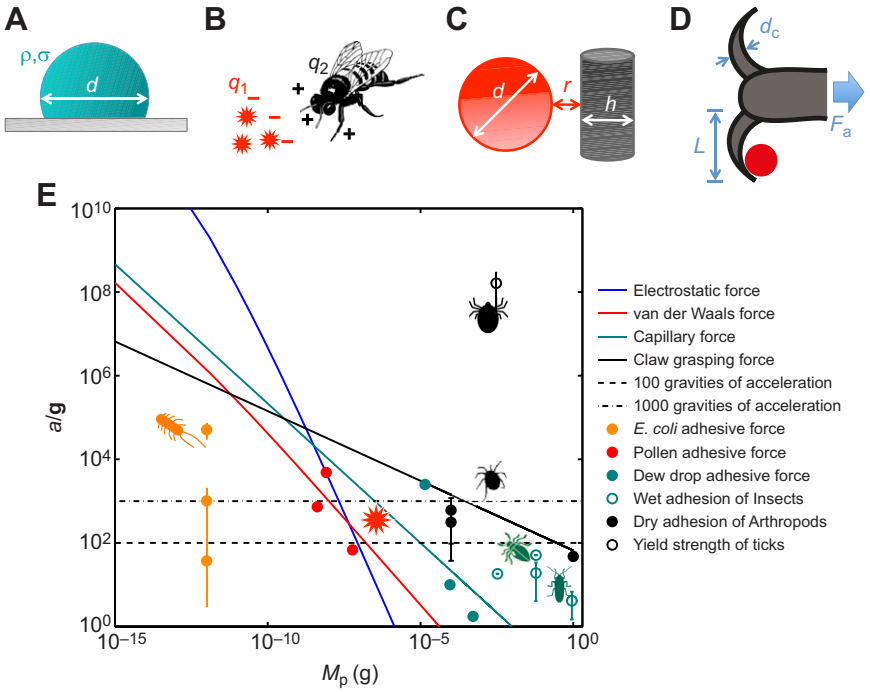

Fig. 5. Modeling aerosol adhesion. Schematics of (A) capillary interaction between a surface and a water drop with diameter d, density ρ and surface tension σ, (B) electrostatic interaction between pollen with a charge q_1 and a honeybee with a charge q_2, (C) van der Waals interaction between a particle of diameter d and hair filament of thickness h with a gap r between them, and (D) claw with length L and diameter d_c bending under the applied force F_a. (E) Relationship between particle mass (M_p) and dimensionless acceleration ($a/\boldsymbol{g}$) required to remove the particle. The removal acceleration a is normalized by gravitational acceleration $\boldsymbol{g}$. Lines correspond to predictions from mathematical modeling, given by Eqns 2–5. Previously reported adhesion forces for various particles (pollen), pests (*E. coli*, mites, ticks) and insects with wet foot pads (beetles, cockroaches, flies, aphids) are also shown (Walker, 1993; Vaknin et al., 2000; Seidl, 2002; Kesel et al., 2003; Vadillo-Rodriguez et al., 2004; Heethoff and Koerner, 2007; Boks et al., 2008; Dickerson and Hu, 2014). Silhouettes obtained from Flaticon.com.

remove the particle. This acceleration is reported in a dimensionless fashion, in terms of the number of gravities $\boldsymbol{g}$. Fig. 5E shows the dimensionless acceleration $a/\boldsymbol{g}$ required for removal of a variety of particles, including liquid drops, pollen, bacteria and mites. These data were collected from previous experiments (Walker, 1993; Vaknin et al., 2000; Kesel et al., 2003; Vadillo-Rodriguez et al., 2004; Heethoff and Koerner, 2007; Boks et al., 2008; Dickerson and Hu, 2014). If attachment force was reported, we divided by particle weight $M_p\boldsymbol{g}$ to calculate the associated dimensionless acceleration. Since common particles such as pollen grains have a density ρ_{pollen}=1.3 g cm^{-3}, which is close to that of water, we assume particles have a density equal to that of water.

Adhesive forces include intermolecular van der Waals forces, electrostatic forces, and, if water is present, capillary forces (Walton, 2008). We calculate these adhesive forces and compare them with experimental measurements. For simplicity of calculation, we assume all surfaces are smooth. We also assume interactions are between single particles and single hairs. This represents a lower bound for attachment force. In reality, particles wider than the hair-to-hair spacing will exhibit higher adhesion forces since they may touch multiple hairs. The resulting higher contact area can increase adhesion, for example by van der Waals forces, which are proportional to contact area.

Consider a water drop of diameter d emplaced on an animal's surface, as shown in Fig. 5A. Balancing the drop's capillary force σd with its inertia $\rho d^3 a_{st}$ provides the critical acceleration of the drop as a function of its size,

$$a_{st} \sim \frac{\sigma}{\rho d^2}, \quad (2)$$

where σ is the surface tension of water, and ρ is the density of water. This trend, as a function of drop mass $M_p \sim \rho d^3$, is given by the green line in Fig. 5E. For this scaling and all others in this section, we assume a pre-factor of unity. The green filled circles represent drops removed by mosquitoes either shaking their wings or falling to the ground (Dickerson and Hu, 2014). The green open circles represent forces required to pull off insects possessing wet foot pads from planar surfaces (Walker, 1993). Agreement between these experiments and the prediction is good.

Flying insects and pollen may develop an opposing electrical charge. This difference in charge gives rise to an attractive electrostatic force (Vaknin et al., 2000) given by Coloumb's law, $F=(k_e q_1 q_2)/(d+h)^2$, where k_e is Coulomb's constant (k_e=9×10^{18} ergs cm C^{-2}), q_1 and q_2 are the charge magnitudes of the particle and organism, respectively [e.g. q_1=0.58±0.26 femtocoulombs for pollen (Bowker and Crenshaw, 2007), q_2=100±80 picocoulombs for honeybees and flies (Vaknin et al., 2000; Ortega-Jimenez and Dudley, 2013)] and h is the width of the structure attracting the particle (e.g. diameter of an individual hair). This law treats animals and particles as charged points, as shown in Fig. 5B. The

Table 2. Measured allometric relationships for hair and bristles of mammals and insects

	Variable	Unit	Best fit	R^2	n	LCI	UCI
Surface area (without hairs)	A_{body}	cm^2	1.7 $M_b^{0.53}$	0.82	27	0.43	0.63
Surface area (with hairs)	A_{hair}	cm^2	83 $M_b^{0.63}$	0.63	27	0.43	0.82
Number of hairs	N	–	4.0×10^6 $M_b^{0.20}$	0.15	27	0.00	0.40
Density of hairs	η	cm^{-2}	2.5×10^5 $M_b^{-0.33}$	0.42	27	–0.48	–0.17
Diameter of hairs	h	cm	180 $M_b^{0.081}$	0.32	27	0.03	0.13
Length of hairs	L	cm	73 $M_b^{0.35}$	0.72	27	0.26	0.43

Body mass M_b is given in grams. Here, n is the sample size, and LCI and UCI are the lower and upper 95% confidence intervals, respectively.

acceleration required to overcome the electrostatic force is

$$a_{es} = \frac{k_e q_1 q_2}{\rho d^3 (d+h)^2}. \quad (3)$$

The blue line in Fig. 5E shows the acceleration required to remove a particle of mass M_p, assuming values for q_1 and q_2 equal to the mean of the values given previously and $h \approx 2$ µm for insects. Electrostatic force is used by honeybees to dislodge pollen from plants (Vaknin et al., 2000).

The intermolecular van der Waals force is expressed in terms of the sum of energy potentials between individual atoms (Israelachvili, 2011). The force between two arbitrary bodies is found by integrating across all points within each of the bodies. Thus, van der Waals forces depend intimately on the shapes of the bodies under consideration. Using a model derived by Rosenfeld and Wasan (1974), we consider a spherical particle and a cylinder, representing a hair, as shown in Fig. 5C. The acceleration to overcome the van der Waals force is:

$$a_{vw} = \frac{2H}{3\rho(d+h)^2 r^2}\sqrt{\frac{h}{h+d+2r}}, \quad (4)$$

where H is the Hamaker constant [taken as 4×10^{-13} ergs (Israelachvili, 2011)], h is the thickness of the hair ($h \approx 2$ µm) and r is the atomic gap between the particle and hair, which depends on the roughness of each. For our scaling, we use $r=1$ nm following a study of sand accumulating onto cilia of desert spiders (Duncan et al., 2007). The Hamaker constant H accounts for the interaction between atoms of the two surfaces and depends on the concentration of atoms and their intermolecular interactions. The red line in Fig. 5E shows the acceleration required to eject a particle of mass M_p. The three red closed circles represent van der Waals forces between common pollen and plants (Vaknin et al., 2000), which closely match our predictions.

Electrostatic and van der Waals forces each have distances at which they are dominant. Walton considered such distances for a 10 µm particle under dry conditions (Walton, 2008). For distances over 0.1 µm, electrostatic forces from the net charge on the particles may dominate. For distances between 10 and 100 nm, electrostatic forces from local charge patches on the surface may dominate. For distances of less than 10 nm, van der Waals forces dominate.

Arthropods, like beetles and mites, push the envelope of attainable attachment force. They have evolved claws to grasp surface asperities. The strength of attachment is dictated by the maximum moment, or torque, that the claw can resist before breaking. The schematic in Fig. 5D shows an arthropod's tarsal claw resisting an applied force F_a by gripping an asperity. The maximum bending moment M_{max} experienced by the claw is $M_{max}=F_a L$, where L is the claw length. Following Euler–Benoulli beam theory, the maximum stress σ_{max} that a deformed beam can withstand may be expressed as $\sigma_{max}=(d_c M_{max})/I$ (Roylance, 2000). Here, d_c represents the average diameter of the claw and $I \sim d_c^4$ is the second moment of area of the cross section of the claw, here assumed to be a circular beam. Thus, the maximum force the claw can resist is $F_a=(\sigma_{max} I)/(d_c L)$. If the claw grows isometrically, then its length and diameter scale as $L \sim d \sim M_p^{1/3}$. The acceleration that will break the claw may be written:

$$a_{cl} \sim \frac{\sigma_{max}}{\rho d_c}. \quad (5)$$

Dai and co-workers report that the maximum stress for a beetle claw, a composite structure comprising both stiff exocuticle and soft endocuticle, is $\sigma_{max}=413.8$ N mm^{-2} (Dai et al., 2002). The black line in Fig. 5E shows how the acceleration varies with pest size M_p. The two black filled circles show the acceleration required to break the claws of mites (Heethoff and Koerner, 2007) and beetles (Dai et al., 2002). Mites and beetles may be considered ectoparasitic because they cling on to larger host animals (Peck, 2006).

In this section, we calculated the attachment forces depending on the material properties of the surfaces and the contact areas involved. In the next sections, we enumerate the methods by which animals generate the forces to exceed these attachment forces and remove particles.

Non-renewable cleaning

The term non-renewable cleaning encompasses all processes that rely on an organism's energy. We now discuss each method in turn.

Brushing with bristled appendages

When we brush our hair, we transfer lint, dandruff and loose hair strands to a hairbrush. Similarly, insects carry brushes that they use to pick up accumulated particles. After brushing, they use a separate technique to clean their 'brush'. An illustration of the process involved when an insect combs its hair is shown in Fig. 6A. Physically, brushing uses frictional and normal forces to overcome a particle's adhesion to the body. The coefficient of friction between a bristled limb and a particle dictates the frictional force, while limb kinematics dictate the normal force. Brushing with bristled appendages is effective for removing particles nestled within hairs.

Honeybees brush themselves with sophisticated bristled structures, shown in Fig. 2, to remove and then package accumulated pollen grains (Thorp, 1979; Winston, 1991). The eyes, wings, and antennae (Fig. 2A–C), along with the head and thorax are groomed using the specialized structures of the forelimbs, shown in Fig. 2D. To collect pollen, the forelimbs are then rubbed together to gather and moisten the accumulated pollen with regurgitated nectar. The pollen press on the 'knee' of the hindlimbs is used to clump the pollen. The clumped pollen is then packed onto the hindlimb, as shown in Fig. 2E, and transported back to the hive.

Honeybees may use the same brushing techniques to remove parasitic mites, like *Varroa* and tracheal mites. The mites are sensed by the bees through touch sensors that trigger brushing (Villa, 2006). Effective grooming is critical for preventing the burrowing of tracheal mites, which burrow inside a bee's tracheae approximately 24 h after attaching. Once inside the tracheae, mites obstruct respiration and pierce through the tissue to drink hemolymph, leading to debilitating effects on the bee's muscles. Removing mites before they spread to the hive is critical for survival.

Brushing may involve a surface external to the body. It has also been speculated that the difference in surface energies between hair arrays and the substrate play a role in the transfer of particles for the fibrillar footpads of geckos (Hansen and Autumn, 2005) and insects (Clemente et al., 2010). Surface energy is the excess energy of atoms at the surface, which dictates how attractive the surface is to fluids and small particles. Higher surface energies entail stronger attraction forces. Fibrillar adhesive systems have a low surface energy when compared with most rigid surfaces, so particles prefer to attach to the substrate rather than the footpads. In addition, particles may be removed through shearing forces in the loading, dragging and unloading of fibrillar pads during locomotion (Mengüç et al., 2014). This unique phenomenon has inspired the design of self-cleaning adhesives (Lee and Fearing, 2008; Glinel et al., 2012; Mengüç et al., 2014).

Journal of Experimental Biology (2015) 218, 3164-3174 doi:10.1242/jeb.103937

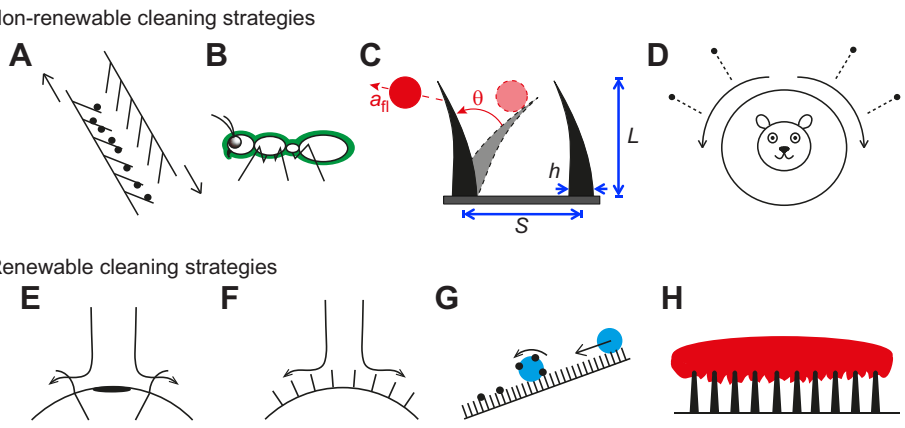

Fig. 6. Cleaning strategies. Schematics of (A–D) non-renewable and (E–H) renewable cleaning techniques. Non-renewable strategies include (A) brushing, (B) secretion, (C) flicking and (D) shaking. Renewable strategies include (E) flow diversion by eyelashes, (F) flow diversion by compound eye hairs, (G) Lotus effect and (H) impalement by nano-structures of cicada wings. The variables in C are: the launching acceleration a_{fl} of a flicked particle, angle θ that the flicked hair traverses, and the hair center-to-center spacing S, thickness h and length L.

Encapsulating with secreted fluids

In this section, we present strategies that use secreted fluids to encapsulate particles and facilitate their transfer. Examples include licking with a tongue, shearing by wet footpads and secretion from special glands. Removal of particles through licking depends on the saliva thickness and its fluid properties, such as surface tension and viscosity. The viscous or capillary forces exerted by saliva during licking need to overcome the adhesive forces of the accumulated particles. Special structures, like the papillae on cat tongues, can also help them to clean more thoroughly.

Licking may also provide antibacterial, thermoregulatory and social benefits. The saliva of humans and rats has been found to have antibacterial properties (Spruijt et al., 1992). This antibacterial property is used in rodents for treating wounds and protecting newborns, who may be vulnerable to infection. Evaporation of saliva on the body can also help to regulate body temperature and serve as a chemical signal to attract mates. Both vertebrates and insects brush and lick (Szebenyi, 1969; Lipps, 1973; Hlavac, 1975; Spruijt et al., 1992). As a last resort, certain animals simply ingest the particles accumulated on the bristled appendages (Szebenyi, 1969; Lipps, 1973). The digestive system packages and ejects the particles through defecation.

When we step on dog feces, a common reaction is to wipe our foot on the ground. Similarly, stick insects and beetles can use a similar shearing motion of their foot to transfer accumulated particles to the substrate (Clemente et al., 2010). The footpad of these animals continually secretes fluid that pushes away particles, making them easier to remove. In fact, particles encapsulated in the footpad's adhesive fluid were found to be left behind during locomotion (Clemente et al., 2010). The combination of secretion and shearing may explain why the wet adhesive pads of insects self-clean more efficiently than the dry pads of geckos (Clemente et al., 2010). Ants also use metapleural glands to secrete chemicals with antibiotic properties (fig. 7B in Beattie et al., 1985). These secretions damage plant pollen and fungal spores, which explains why ants never evolved as successful pollinators, like bees and wasps.

Flicking

We saw previously that hairs on appendages can serve as combs. Hairs on the body can also facilitate particle removal. The erect hairs covering the head and thorax of insects allow for the storage and release of potential energy, thus acting as springboards to catapult accumulated particles, as shown in Fig. 6C. This mechanism uses the inertial force imparted by the accelerating hair to overcome adhesion. The flicking accelerations can be calculated using Euler–Bernoulli beam theory (Ostachowicz and Krawczuk, 1991) for an oscillating beam. The acceleration imparted by one flick may be written:

$$a_{fl} = S\omega_n^2 = \frac{1.875^4 4S}{\pi}\frac{EI}{\rho h^2 L^4}, \quad (6)$$

where ω_n is the first mode of natural frequency of a flicked hair, modeled as a cantilevered beam with a constant diameter h (Ostachowicz and Krawczuk, 1991), EI is its flexural stiffness (Vincent and Wegst, 2004; Vogel, 2013), ρ is the hair's material density (Vincent and Wegst, 2004), L is its length and S is the spacing between the hairs, which dictates the maximum, unimpeded deflection of the hair. Assuming E is independent of body size and substituting scalings for hair length and spacing from Table 2 ($S \sim M_b^{0.16}$, $h \sim M_b^{0.081}$ and $L \sim M_b^{0.35}$), we find $a_{fl} \sim M_b^{-1.1}$. The negative exponent indicates that flicking is more effective for smaller animals. Our experiments show that a fruit fly antenna 250 µm long accelerates at 100–500 ***g***. A honeybee ocular hair flicks particles at 500 ***g***. Thus, hairs act like catapults springing micrometer-sized particles away. The range of acceleration is 100–1000 ***g***, regimes indicated by the dashed horizontal lines in Fig. 5E. This large force is greater than adhesion forces for a number of particles, including pollen, dewdrops and mites. In contrast, the fur of an elk, with 5-cm-long hairs accelerate particles at 1–2 ***g***, which is sufficient to release larger particles that are trapped between hairs, but insufficient for small particles. Eqn 6 predicts values, shown in Table 3, that agree well with our experiments with elk fur and are two orders of magnitude greater for honeybees. The effects of drag at small scales may explain the over-prediction for honeybees.

Table 3. Predicted and measured values for flicked particle accelerations following our mathematical model a_{fl}, Eqn 6 and high-speed videography $a_{fl,exp}$

	ρ (kg m^{-3})	E (MPa)	L (cm)	h (cm)	S (cm)	ω_n (s^{-1})	a_{fl} (m s^{-2})	$a_{fl,exp}$ (m s^{-2})
Elk	1300	9000	4.9	0.01	0.35	94	32	18
Honeybee	1	0.2	0.025	7.0×10^{-4}	0.007	4.4×10^{4}	1.5×10^{5}	5000

Hair properties: density ρ, elasticity E, length L, thickness h, and center-to-center spacing S, are from Goldsmith and Baden, 1970; Robbins, 2002; Vincent and Wegst, 2004 and our own measurements.

Flicking is also effective in cleaning the bristled feet of geckos. The bristles beneath the feet of geckos are responsible for the van der Waals adhesion necessary to climb walls and walk upside down. To disengage the bristles, geckos hyper-extend their toes. During hyperextension, the adhesive force between the bristles and the substrate act as a catch that permits the storage of elastic energy in the bristles. Once the bristles disengage, the bristles fling outwards, catapulting particles (Hu et al., 2012). When 10–20% of the footpad bristles are in contact with the substrate, the released elastic energy can impart 68–120 $\boldsymbol{g}$ of acceleration onto 10 µm particles (Hu et al., 2012).

A strategy similar to the flicking observed in animal hair has been developed for micro-manipulation (Haliyo et al., 2003). Previous workers used a cantilevered micro-beam to capture small particles ($d_p \approx 40$–80 µm) and then designed a piezoelectric actuator to flick the micro-beam and impart 10^4 m s^{-2} of acceleration to release the particles. This high acceleration is enough to overcome the adhesive force between the particles and the micro-beam.

Shaking

Animals may use violent body shakes to remove accumulated aerosols (Fig. 6D). Such motions have been found to help mammals, birds and mosquitoes expel accumulated water (Dickerson et al., 2012; Ortega-Jimenez and Dudley, 2012; Dickerson and Hu, 2014). Shaking mammals can impart accelerations of 10–70 $\boldsymbol{g}$ to adhered water (Dickerson et al., 2012). From Dickerson et al., the non-dimensional acceleration a_{sh} during mammalian shaking scales as:

$$a_{sh} \sim M_b^{-1/24}. \quad (7)$$

Flying animals, like hummingbirds and insects may use wing flutters along with shakes to impart high accelerations and remove particles. Hummingbirds can impart accelerations of 10–200 $\boldsymbol{g}$ (Ortega-Jimenez and Dudley, 2012), while mosquitoes can impart accelerations up to 2500 $\boldsymbol{g}$ (Dickerson and Hu, 2014). By combining bathing with shaking, mammals and birds can use the wetting properties of water to overcome the particles' adhesion and then use the centrifugal forces from shaking motions to remove both water and particles.

Shaking and flicking generate 100–1000 $\boldsymbol{g}$ of acceleration, which is in the regime of the required acceleration to remove most aerosols such as pollen, water drops, insects and mites. Bacteria are too lightweight, weighing 10^{-12} g, and so require an implausible 10^4 $\boldsymbol{g}$ to shake off. Ticks possess such strong mouthparts that they require 10^8 $\boldsymbol{g}$ to remove once latched on (Seidl, 2002; Kesel et al., 2003). Such organisms are beyond the range of accelerations that can be generated by animals and are removed through scratching or biting.

Washing machines use a spin cycle to remove water from clothes and reduce the drying time. Similar to the wet-dog shake, the centrifugal forces generated by spinning act to overcome the capillary forces between water and clothes. Modern washing machines spin at upwards of 800 rpm and normally have a drum with a radius of ∼30 cm (Akcabay, 2007), thus generating approximately 200 $\boldsymbol{g}$ of acceleration, enough to remove small particles and water drops with a diameter d=20 µm or greater, which is calculated from Eqn 2.

Similarly, small sensors, like charge-coupled devices (CCDs) in digital cameras, vibrate at high frequencies to remove accumulated dust (Timacheff, 2011). Two different strategies have been patented by Olympus (Takizawa and Kawai, 2008) and Konica Minolta (Okumura et al., 2010). The Olympus system, called the Supersonic Wave Filter™, vibrates a transparent foil that covers the camera's sensors at frequencies above 20 kHz. The Minolta system vibrates the actual sensor at around 100 Hz through large amplitude. To remove particles of diameter d=20 µm adhered by electrostatic or van der Waals force, these dust-removal devices would have to generate 1000 $\boldsymbol{g}$ of acceleration, according to Eqns 3 and 4. Such acceleration would require the Olympus Supersonic Wave Filter™ to vibrate at an amplitude of only 2.5×10^{-3} cm, while the Minolta system would have to vibrate at an amplitude of 100 cm. The amplitude for the Minolta is likely to be much smaller, making it less effective than the Olympus.

Renewable cleaning

If prevention is better then cure, then renewable is better than non-renewable cleaning. In renewable cleaning, surface structure and chemistry are key and no specialized movements are required once such structures are in place. Instead, organisms exploit external, renewable sources like wind and rain to prevent soiling and facilitate cleaning.

Reduction of deposition by diverting airflow

Mammalian eyelashes protect the eye by minimizing airflow across the eye surface, as shown in Fig. 6E (Amador et al., 2015). The shear stress τ that the surrounding airflow exerts onto the eye surface is positively correlated with the contamination of the tear film (Schneider and Bohgard, 2005; Amador et al., 2015). Using viscous flow theory, we can predict how this shear stress is affected by the presence of eyelashes, and how it varies with eyelash length L, or:

$$\tau \sim aL^{-1} + bL^2. \quad (8)$$

Here, a and b are constants dependent on fluid properties and eye geometry (Amador et al., 2015). The two terms of this expression correspond to contributions from short eyelashes and long lashes. For short lashes, the boundary layer at the eye surface is thickened because of the flow resistance imposed by the lashes and so the shear stress approximately scales as $\tau \sim L^{-1}$. Long eyelashes protrude further into the surrounding airflow and channel high-velocity airflow towards the eye; therefore, the shear stress scales as $\tau \sim L^2$. The competition between these two effects results in an intermediate optimal eyelash length L/W=0.3±0.1, where W is the eye's opening width. At this length, eyelashes reduce particle deposition by 50%. Measurements of 22 genetically diverse mammalian species, from hedgehogs to giraffes, indicate eyelash length is tuned by evolutionary pressures to a length of approximately one-third the eye width, or L/W=0.38±0.15.

The compound eyes of many species of insects are covered by an array of short hairs evenly spaced between each lens, or ommatidium, as shown in Fig. 2A. These hairs, like eyelashes, keep compound eyes clean by diverting airflow, as illustrated in Fig. 6F (G.J.A., unpublished results). The hairs create a stagnant zone in front of the eye, but, because they are not circumferential, do not channel airflow if they are long. Therefore, the shear stress τ at the eye surface for insect eyes scales like the first term in Eqn 8, or $\tau \sim L^{-1}$. Increasing hair length has minimal benefits beyond a length L=S, where S is the center-to-center spacing of the hairs. Numerical simulations and wind tunnel experiments using an insect eye mimic show this hair length reduces shear rate at the eye surface by 90%. Among 17 insect species studied, hair length L is approximately equal to spacing S.

Surface patterning

In the lotus effect, raindrops roll across the surface of a lotus leaf, picking up deposited particles, as shown in Fig. 6G (Barthlott and Neinhuis, 1997). Water beads up on rough, structured surfaces because it requires more energy for the water droplet to cover all of the nooks and crannies than to simply rest on top of the surface features (Blossey, 2003). The lotus effect has also been observed for the fibrillar pads of geckos (Autumn and Hansen, 2006). This ability has inspired development of super hydrophobic coatings for keeping surfaces clean (Blossey, 2003; Wong et al., 2011), as well as mushroom-shaped microfibrillar adhesives that can be completely cleaned by rolling water drops (Kim et al., 2009). The use of super hydrophobic surfaces has even been extended to preventing bacterial growth (Glinel et al., 2012).

The sharp points on the wings of cicadas act like pincushions and the bacteria sit atop them like water balloons (Fig. 6H). The nanostructures on the wings stretch the cell membranes of bacteria causing them to rupture (Pogodin et al., 2013). The nanostructures do not prevent adhesion like the lotus leaf. In fact, they exploit adhesion in order to rupture and kill the bacteria. A synthetic counterpart of cicada wings has been found in black silicon. The high-aspect ratio nanostructures on its surface exhibit bacteria killing rates similar to cicada wings, approximately 450,000 cells min^{-1} cm^{-2} (Ivanova et al., 2013).

Instead of making surfaces into pincushions, an alternate technique is to make them ultra-smooth. The hairs of golden moles are exceedingly smooth, unlike hairs of humans and other mammals, which are rough. The smoothness of mole hairs is due to the compression of cuticular scales on the hair's surface (Snyder et al., 2012). These smooth hairs are hypothesized to help streamline locomotion in dirt and sand, as well as maintain cleanliness through their lower surface area. Additionally, the smooth leaves of certain plants may help wind to blow away accumulated airborne seeds and spores (Vogel, 2012). By keeping their protruding veins underneath and having a smooth upper surface, leaves provide minimal shelter for spores and seeds to hide from the wind.

Perspectives

We clean every day. In the US, we spend 0.33% of our lives bathing and 2.9% cleaning our houses (US Department of Labor, 2014). We are faster than our ancestors because of technology such as brushes, cloths and vacuum cleaners. In this Review, we show that cleaning is a fundamental part of life. Animals spend a great deal of time cleaning themselves. Just watch most mammals, birds or even houseflies. They are meticulous in their activities. Just as humans have invented technology to make cleaning more energetically efficient and faster, so have insects evolved their own methods.

Cleaning an animal is not as simple as wiping a tabletop. Animals ranging from insects to bears have hair. Hair can increase the surface area of an animal by one hundred times. While animals probably evolved this hair as insulation, they also bear the burden of creating more surface area to clean. Certain types of hair can ease this burden by facilitating cleaning. Eyelashes, for example, prevent dust accumulation on the eye by diverting airflow. Hairs can act as catapults, flicking off small particles at high acceleration when triggered. Such methods especially target the smallest particles because these are the most difficult to remove.

In the limited space of this Review, we left a great number of animals unstudied. For example, how underwater animals such as fish prevent fouling is not well understood. The feathers of birds also present an enormous surface area that needs to be cleaned. We do not have measurements of the kinematics of the grooming motions for most animals. We are also missing metrics such as efficiency to describe cleaning. Clearly, cleaning increases fitness and it does so at an energy cost. But given this energetic cost, how often should an animal clean itself? Why do we clean our homes and cities with a certain frequency? The energy–utility tradeoff of cleaning is not well understood.

We have reviewed techniques for particle removal, but similar techniques exist for self-soiling. This is a fascinating but understudied area. It may have applications in creating better wipes for everyday use. Certain species of desert-dwelling spiders have developed techniques for coating themselves with sand in order to camouflage themselves (Duncan et al., 2007). In honeybees, the branched hairs on the thorax attract pollen grains during foraging (Thorp, 1979). Rather than preventing the accumulation of particles, this strategy utilizes nano-scale hair lettes to maximize surface area and adhesion force. In order to feed their larvae, certain species of bees have developed specialized 'mopping' hair structures to absorb and capture fatty oils from plants (Vogel, 1981). These specialized hairs generate high capillary forces that suck up fatty oils secreted by plants. In addition to these absorptive structures, the bees developed structures to extract these oils from their hairs when feeding their larvae.

Self-cleaning technologies have received much attention, especially with the progression of autonomous robots and microelectromechanical systems (MEMS). MEMS devices rely heavily on the precise calibration of their sensing microcantilevers. The slightest bit of particle deposition could greatly affect the accuracy of the data obtained because of the cantilevers' low mass and high sensitivity. Current self-cleaning designs rely on unique geometrical attributes that prevent the accumulation of particles, like micro grooved surfaces that push particles away from contact surfaces (Shi and Kim, 2005). Drones, as well as other autonomous technologies like rovers, rely on cameras for operation and solar panels for energy. With prolonged exposure to environmental conditions, the sensitive equipment on drones and rovers are susceptible to failure due to soiling. After the Mars Exploration Rover experienced a blackout when its solar panels were covered in dust and dirt, technology was suggested to prevent such failures (Calle et al., 2008; Walton, 2008). One technology currently being pursued relies on electrostatic coatings, which generate fluctuating electrical forces to dislodge and remove deposited particles (Calle et al., 2008).

Understanding how biological systems, like eyelashes, prevent soiling by interacting with the environment can help inspire low-energy solutions for keeping sensitive equipment free from soiling. Bio-inspired renewable cleaning strategies based on surface structure or chemistry have been previously developed (Glinel et al., 2012; Liu and Jiang, 2012), such as super hydrophobic and super hydrophilic coatings, algae-inspired layers that prevent cell-to-cell communication and synthetic bactericidal coatings. However, in general, non-renewable strategies are more often put into application. Further development and implementation of renewable technologies may one day improve biomedical, marine and industrial engineering and benefit society.

The phrase 'cleanliness is next to godliness' has ancient roots. In fact, many religions have elaborate washing rituals, which had the unintended effect of improving human hygiene far before the discovery of microbes. Cleanliness will always be a part of religion, but it is also playing an increasing role in the sciences. On our planet, we are now faced with clear evidence that human carbon dioxide production is causing changes in the climate. In the coming years, we will likely experience greater amounts of smog, pollutants,

Journal of Experimental Biology

pesticides and other aerosols. Little is known about how these particulates affect animal and plant life. Some of it may already be affecting the population of honeybees, which are of critical importance to agriculture, but whose decline remains undetermined. A fundamental understanding of cleaning may help us bravely cope with this new world, as well as educate ourselves on the limits of the organisms on which our lives depend.

Acknowledgements
We thank F. Durand, D. Waller and E. Jung for their contributions.

Competing interests
The authors declare no competing or financial interests.

Funding
We acknowledge financial support from the National Science Foundation [grant no. PHY-1255127 and CBET-1510884].

References

Akcabay, D. T. (2007). *Physics Based Washing Machine Simulations*. PhD thesis, University of Michigan.
Amador, G. J., Mao, W., DeMercurio, P., Montero, C., Clewis, J., Alexeev, A. and Hu, D. L. (2015). Eyelashes divert airflow to protect the eye. *J. R. Soc. Interface* **12**, 20141294.
Autumn, K. and Hansen, W. (2006). Ultrahydrophobicity indicates a non-adhesive default state in gecko setae. *J. Comp. Physiol. A* **192**, 1205-1212.
Autumn, K., Sitti, M., Liang, Y. A., Peattie, A. M., Hansen, W. R., Sponberg, S., Kenny, T. W., Fearing, R., Israelachvili, J. N. and Full, R. J. (2002). Evidence for van der Waals adhesion in gecko setae. *Proc. Natl. Acad. Sci. USA* **99**, 12252-12256.
Barthlott, W. and Neinhuis, C. (1997). Purity of the sacred lotus, or escape from contamination in biological surfaces. *Planta* **202**, 1-8.
Beattie, A. J., Turnbull, C., Hough, T., Jobson, S. and Knox R. B. (1985). The vulnerability of pollen and fungal spores to ant secretions: evidence and some evolutionary implications. *Am. J. Bot.* **72**, 606-614.
Bejan, A. (1990). Theory of heat transfer from a surface covered with hair. *J. Heat Transfer* **112**, 662-667.
Blossey, R. (2003). Self-cleaning surfaces - virtual realities. *Nat. Mater.* **2**, 301-306.
Boks, N. P., Norde, W., van der Mei, H. C. and Busscher, H. J. (2008). Forces involved in bacterial adhesion to hydrophilic and hydrophobic surfaces. *Microbiology* **154**, 3122-3133.
Bourouiba, L., Dehandschoewercker, E. and Bush, J. W. M. (2014). Violent expiratory events: on coughing and sneezing. *J. Fluid Mech.* **745**, 537-563.
Bowker, G. E. and Crenshaw, H. C. (2007). Electrostatic forces in wind-pollination Part 1: measurement of the electrostatic charge on pollen. *Atmosph. Environ.* **41**, 1587-1595.
Calder, W. A. (1996). *Size, Function, and Life History*. Mineola, NY: Courier Dover Publications.
Calle, C., McFall, J. et al. (2008). Dust particle removal by electrostatic and dielectrophoretic forces with applications to NASA exploration missions. Proceedings of the Electrostatics Society of America Annual Meeting, Minneapolis, 17-19.
Carlson, S. D. and Chi, C. (1974). Surface fine structure of the eye of the housefly (*Musca domestica*): ommatidia and lamina ganglionaris. *Cell Tissue Res.* **149**, 21-41.
Casas, J., Steinmann, T. and Krijnen, G. (2010). Why do insects have such a high density of flow-sensing hairs? Insights from the hydromechanics of biomimetic MEMS sensors. *J. R. Soc. Interface* **7**, rsif20100093.
Clemente, C. J., Bullock, J. M. R., Beale, A. and Federle, W. (2010). Evidence for self-cleaning in fluid-based smooth and hairy adhesive systems of insects. *J. Exp. Biol.* **213**, 635-642.
Conley, K. E. and Porter, W. P. (1986). Heat loss from deer mice (*Peromyscus*): evaluation of seasonal limits to thermoregulation. *J. Exp. Biol.* **126**, 249.
Dai, Z., Gorb, S. N. and Schwarz, U. (2002). Roughness-dependent friction force of the tarsal claw system in the beetle *Pachnoda marginata* (Coleoptera, Scarabaeidae). *J. Exp. Biol.* **205**, 2479-2488.
Dickerson, A. K. and Hu, D. L. (2014). Mosquitoes actively remove drops deposited by fog and dew. *Integr. Comp. Biol.* **54**, 1008-1013.
Dickerson, A. K., Mills, Z. G. and Hu, D. L. (2012). Wet mammals shake at tuned frequencies to dry. *J. R. Soc. Interface* **9**, 3208-3218.
Duncan, R. P., Autumn, K. and Binford, G. J. (2007). Convergent setal morphology in sand-covering spiders suggests a design principle for particle capture. *Proc. R. Soc. B Biol. Sci.* **274**, 3049-3057.
Estes, J. A. (1980). *Enhydra lutris*. *Mamm. Species* **133**, 1-8.
Federle, W. (2006). Why are so many adhesive pads hairy? *J. Exp. Biol.* **209**, 2611-2621.
Fedosenko, A. K. and Blank, D. A. (2005). *Ovis ammon*. *Mamm. Species* **773**, 1-15.
Fish, F. E., Smelstoys, J. et al. (2002). Fur does not fly, it floats: buoyancy of pelage in semi-aquatic mammals. *Aquat. Mamm.* **28**, 103-112.
Glinel, K., Thebault, P., Humblot, V., Pradier, C. M. and Jouenne, T. (2012). Antibacterial surfaces developed from bio-inspired approaches. *Acta Biomater.* **8**, 1670-1684.
Goldsmith, L. A. and Baden, H. P. (1970). The mechanical properties of hair I. The dynamic sonic modulus. *J. Invest. Dermatol.* **55**, 256-259.
Haliyo, D. S., Régnier, S. and Bidaud, P. (2003). Manipulation of micro-objects using adhesion forces and dynamical effects. *Exp. Robot. VIII* **5**, 382-391.
Hansen, W. R. and Autumn, K. (2005). Evidence for self-cleaning in gecko setae. *Proc. Natl. Acad. Sci. USA* **102**, 385-389.
Heethoff, M. and Koerner, L. (2007). Small but powerful: the oribatid mite *Archegozetes longisetosus* Aoki (Acari, Oribatida) produces disproportionately high forces. *J. Exp. Biol.* **210**, 3036-3042.
Hlavac, T. F. (1975). Grooming systems of insects: structure, mechanics. *Ann. Entomol. Soc. Am.* **68**, 823-826.
Holdgate, M. (1955). The wetting of insect cuticles by water. *J. Exp. Biol.* **32**, 591-617.
Hu, S., Lopez, S., Niewiarowski, P. H. and Xia, Z. (2012). Dynamic self-cleaning in gecko setae via digital hyperextension. *J. R. Soc. Interface* **9**, 2781-2790.
Israelachvili, J. N. (2011). *Intermolecular and Surface Forces*. Oxford, UK: Academic Press.
Ivanova, E. P., Hasan, J., Webb, H. K., Gervinskas, G., Juodkazis, S., Truong, V. K., Wu, A. H. F., Lamb, R. N., Baulin, V. A., Watson, G. S. et al. (2013). Bactericidal activity of black silicon. *Nat. Commun.* **4**, 2838.
Jenkins, S. H. and Busher, P. E. (1979). *Castor canadensis*. *Mamm. Species* **120**, 1-8.
Kesel, A. B., Martin, A. and Seidl, T. (2003). Adhesion measurements on the attachment devices of the jumping spider *Evarcha arcuata*. *J. Exp. Biol.* **206**, 2733-2738.
Kim, S., Cheung, E. and Sitti, M. (2009). Wet self-cleaning of biologically inspired elastomer mushroom shaped microfibrillar adhesives. *Langmuir* **25**, 7196-7199.
Koprowski, J. L. (1994). *Sciurus carolinensis*. *Mamm. Species* **480**, 1-9.
Kumar, E. S. and Sarkar, B. (2013). Soiling and dust impact on the efficiency and the maximum power point in the photovoltaic modules. *Int. J. Eng.* **2**, 1-8.
Larivière, S. and Walton, L. R. (1998). *Lontra canadensis*. *Mamm. Species* **587**, 1-8.
Lee, J. and Fearing, R. S. (2008). Contact self-cleaning of synthetic gecko adhesive from polymer microfibers. *Langmuir* **24**, 10587-10591.
Lipps, K. L. (1973). *Comparative Cleaning Behavior in Drosophila*. PhD thesis, Davis: University of California.
Liu, K. and Jiang, L. (2012). Bio-inspired self-cleaning surfaces. *Annu. Rev. Mater. Res.* **42**, 231-263.
Mattern, M. Y. and McLennan, D. A. (2000). Phylogeny and speciation of felids. *Cladistics* **16**, 232-253.
Mazumder, M. K., Biris, A. S., Trigwell, S., Sims, R. A., Calle, C. I. and Buhler, C. R. (2003). Solar panel obscuration in the dusty atmosphere of Mars. Proceedings ESA-IEEE Joint Meeting on Electrostatics, 208-218.
McGowan, C. (1994). *Diatoms to Dinosaurs: The Size and Scale of Living Things*. Washington, DC: Island Press.
McMahon, T. A. and Bonner, J. T. (1983). *On Size and Life*. New York: Scientific American Library.
McManus, J. J. (1974). *Didelphis virginiana*. *Mamm. Species* **40**, 1-6.
Mecklenburg, L., Linek, M. and Tobin, D. J. (2009). *Hair Loss Disorders in Domestic Animals*. Wiley-Blackwell.
Mengüç, Y., Röhrig, M., Abusomwan, U., Holscher, H. and Sitti, M. (2014). Staying sticky: contact self-cleaning of gecko-inspired adhesives. *J. R. Soc. Interface* **11**, 20131205.
Neese, V. (1965). Zur Funktion der Augenborsten bei der Honigbiene. *Z. Vgl. Physiol.* **49**, 543-585.
Neese, V. (1966). Zur Bedeutung der Augenborsten bei der Fluggeschwindigkeitsregulation der Bienen. *Z. Vgl. Physiol.* **52**, 149-154.
Okumura, Y., Watanabe, Y. and Mikami, K. (2010). Image pickup apparatus controlling shake sensing and/or shake compensation during dust removal. US patent no. US7680403 B2.
Olsen, P. (1983). Water-rat *Hydromys chrysogaster*. In *The Australian Museum Complete Book of Australian Mammals* (ed. R. Strahan), pp. 367-368. Chatswood, Australia: Reed Books.
Ortega-Jimenez, V. M. and Dudley, R. (2012). Aerial shaking performance of wet Anna's hummingbirds. *J. R. Soc. Interface* **9**, 1093-1099.
Ortega-Jimenez, V. M. and Dudley, R. (2013). Spiderweb deformation induced by electrostatically charged insects. *Sci. Rep.* **3**, 2108.
Ostachowicz, W. M. and Krawczuk, M. (1991). Analysis of the effect of cracks on the natural frequencies of a cantilever beam. *J. Sound Vib.* **150**, 191-201.
Pasitschniak-Arts, M. and Marinelli, L. (1998). *Ornithorhynchus anatinus*. *Mamm. Species* **585**, 1-9.
Pass, D. and Freeth, G. (1993). The rat. *Anzccart News* **6**, 1-4.

Peck, S. B. (2006). Distribution and biology of the ectoparasitic beaver beetle *Platypsyllus castoris* Ritsema in North America (Coleoptera: Leiodidae: Platypsyllinae). *Insecta Mundi* **20**, 85-94.
Pogodin, S., Hasan, J., Baulin, V. A., Webb, H. K., Truong, V. K., Phong Nguyen, T. H., Boshkovikj, V., Fluke, C. J., Watson, G. S., Watson, J. A. et al. (2013). Biophysical model of bacterial cell interactions with nanopatterned cicada wing surfaces. *Biophys. J.* **104**, 835-840.
Robbins, C. R. (2002). *Chemical and Physical Behavior of Human Hair*. Berlin, Germany: Springer.
Rosenfeld, J. I. and Wasan, D. T. (1974). The London force contribution to the van der Waals force between a sphere and a cylinder. *J. Colloid Interface Sci.* **47**, 27-31.
Roylance, D. (2000). Stresses in Beams. http://ocw.mit.edu.
Sammataro, D., Gerson, U. and Needham, G. (2000). Parasitic mites of honey bees: life history, implications, and impact. *Annu. Rev. Entomol.* **45**, 519-548.
Sato, K., Takahashi, H., Nguyen, M. D., Matsumoto, K. and Shimoyama, I. (2013). Effectiveness of Bristled Wing of Thrips. 2013 IEEE 26th International Conference on Micro Electro Mechanical Systems (MEMS), 21-24.
Schmidt-Nielsen, K. (1984). *Scaling: Why is Animal Size So Important?* Cambridge, UK: Cambridge University Press.
Schneider, T. and Bohgard, M. (2005). Airborne particle deposition onto the ocular surface. *Indoor Air* **15**, 215-219.
Scott, D. W., Miller, W. H. and Griffin, C. E. (2001). *Muller and Kirk's Small Animal Dermatology*. Philadelphia, PA: Saunders.
Seidl, T. (2002). *Neue ansätze zur charakterisierung biologischer werkstoffe am beispiel der arthropodenkutikula*. Saarbrücken, Germany: Saarland University.
Shi, Y. and Kim, S.-G. (2005). A lateral, self-cleaning, direct contact MEMS switch. Micro Electro Mechanical Systems, 2005. MEMS 2005. 18th IEEE International Conference on: 195-198.
Sidorovich, V., Kruuk, H. and Macdonald, D. W. (1999). Body size, and interactions between European and American mink (*Mustela lutreola* and *M. vison*) in Eastern Europe. *J. Zool.* **248**, 521-527.
Snyder, H. K., Maia, R., D'Alba, L., Shultz, A. J., Rowe, K. M. C., Rowe, K. C. and Shawkey, M. D. (2012). Iridescent colour production in hairs of blind golden moles (Chrysochloridae). *Biol. Lett.* **8**, rsbl20111168.
Spotorno, A. E., Zuleta, C. A., Valladares, J. P., Deane, A. L. and Jiménez, J. E. (2004). *Chinchilla laniger*. *Mamm. Species* **758**, 1-9.
Spruijt, B., van Hooff, J. and Gispen, W. H. (1992). Ethology and neurobiology of grooming behavior. *Physiol. Rev.* **72**, 825-852.
Szebenyi, A. L. (1969). Cleaning behaviour in *Drosophila melanogaster*. *Anim. Behav.* **17**, 641-651.
Takizawa, H. and Kawai, S. (2008). Camera and image pick-up device unit having an optical member that is vibrated to remove dust. US patent no. US7280145 B2.
Thorp, R. W. (1979). Structural, behavioral, and physiological adaptations of bees (Apoidea) for collecting pollen. *Ann. Missouri Bot. Garden* **66**, 788-812.
Timacheff, S. (2011). *Canon EOS Digital Photography Photo Workshop*. Hoboken, NJ: John Wiley & Sons.
US Department of Labor (2014). **Bureau of Labor Statistics**. American Time Use Survey - 2013 Results. http://www.bls.gov/news.release/pdf/atus.pdf.
US Environmental Protection Agency (2013). Air Quality Statistics Report. http://www.epa.gov/airquality/.
US Environmental Protection Agency (2014). National Summary of Particulate Matter Emissions. http://www.epa.gov/.
Vadillo-Rodriguez, V., Busscher, H. J., Norde, W., de Vries, J. and van der Mei, H. C. (2004). Atomic force microscopic corroboration of bond aging for adhesion of *Streptococcus thermophilus* to solid substrata. *J. Colloid Interface Sci.* **278**, 251-254.
Vaknin, Y., Gan-Mor, S., Bechar, A., Ronen, B. and Eisikowitch, D. (2000). The role of electrostatic forces in pollination. *Plant Syst. Evol.* **222**, 133-142.
Valencak, T. G., Arnold, W., Tataruch, F. and Ruf, T. (2003). High content of polyunsaturated fatty acids in muscle phospholipids of a fast runner, the European brown hare (*Lepus europaeus*). *J. Comp. Physiol. B Biochem. Syst. Environ. Physiol.* **173**, 695-702.
Villa, J. D. (2006). Autogrooming and bee age influence migration of tracheal mites to Russian and susceptible worker honey bees (*Apis mellifera* L). *J. Apicult. Res. Bee World* **45**, 28.
Vincent, J. F. V. and Wegst, U. G. K. (2004). Design and mechanical properties of insect cuticle. *Arthrop. Struct. Dev.* **33**, 187-199.
Vogel, S. (1981). Abdominal oil-mopping - a new type of foraging in bees. *Naturwissenschaften* **68**, 627-628.
Vogel, S. (1983). How much air passes through a silkmoth's antenna? *J. Insect Physiol.* **29**, 597-602.
Vogel, S. (2012). *The Life of a Leaf*. Chicago, IL: The University of Chicago Press.
Vogel, S. (2013). *Comparative Biomechanics: Life's Physical World*. Princeton, NJ: Princeton University Press.
Walker, G. (1993). Adhesion to smooth surfaces by insects: a review. *Int. J. Adhes. Adhes.* **13**, 3-7.
Walton, O. R. (2008). Review of adhesion fundamentals for micron-scale particles. *KONA Powder Particle J.* **26**, 129-141.
Wilcox, H. H. (1950). Histology of the skin and hair of the adult chinchilla. *Anat. Rec.* **108**, 385-397.
Willner, G. R., Feldhamer, G. A., Zucker, E. E. and Chapman, J. A. (1980). *Ondatra zibethicus*. *Mamm. Species* **141**, 1-8.
Wilson, W. E., Spider, L. L., Ellestad, T. G., Lamothe, P. J., Dzubay, T. G., Stevens, R. K., Macias, E. S., Fletcher, R. A., Husar, J. D., Husar, R. B. et al. (1977). General Motors sulfate dispersion experiment: summary of EPA measurements. *J. Air Pollut. Control Assoc.* **27**, 46-51.
Winston, M. L. (1991). *The Biology of the Honey Bee*. Cambridge, MA: Harvard University Press.
Wong, T.-S., Kang, S. H., Tang, S. K. Y., Smythe, E. J., Hatton, B. D., Grinthal, A. and Aizenberg, J. (2011). Bioinspired self-repairing slippery surfaces with pressure-stable omniphobicity. *Nature* **477**, 443-447.